Title
Symmetry Reduction in a Hyperpolarization-Activated Homotetrameric Ion Channel

Journal
Biochemistry, 61(20)

ISSN
0006-2960

Authors
Dickinson, Miles Sasha
Pourmal, Sergei
Gupta, Meghna
et al.

Publication Date
2022-10-18

DOI
10.1021/acs.biochem.1c00654

Peer reviewed

HHS Public Access

Author manuscript

Biochemistry. Author manuscript; available in PMC 2023 February 15.

Published in final edited form as:

Biochemistry. 2022 October 18; 61(20): 2177–2181. doi:10.1021/acs.biochem.1c00654.

Symmetry Reduction in a Hyperpolarization-Activated Homotetrameric Ion Channel

Miles Sasha Dickinson[⊥],
Department of Biochemistry and Biophysics, University of California San Francisco, San Francisco, California 94158, United States; Chemistry and Chemical Biology Graduate Program, University of California San Francisco, San Francisco, California 94143, United States

Sergei Pourmal[⊥],
Department of Biochemistry and Biophysics, University of California San Francisco, San Francisco, California 94158, United States; Chemistry and Chemical Biology Graduate Program, University of California San Francisco, San Francisco, California 94143, United States

Meghna Gupta[⊥],
Department of Biochemistry and Biophysics, University of California San Francisco, San Francisco, California 94158, United States

Maxine Bi,
Department of Biochemistry and Biophysics, University of California San Francisco, San Francisco, California 94158, United States; Graduate Group in Biophysics, University of California San Francisco, San Francisco, California 94143, United States

Robert M. Stroud
Department of Biochemistry and Biophysics, University of California San Francisco, San Francisco, California 94158, United States; Chemistry and Chemical Biology Graduate Program, University of California San Francisco, San Francisco, California 94143, United States; Graduate Group in Biophysics, University of California San Francisco, San Francisco, California 94143, United States

Abstract

Plants obtain nutrients from the soil via transmembrane transporters and channels in their root hairs, from which ions radially transport in toward the xylem for distribution across the plant body.

Corresponding Author: Robert M. Stroud – *Department of Biochemistry and Biophysics, University of California San Francisco, San Francisco, California 94158, United States; Chemistry and Chemical Biology Graduate Program, University of California San Francisco, San Francisco, California 94143, United States; Graduate Group in Biophysics, University of California San Francisco, San Francisco, California 94143, United States*; stroud@msg.ucsf.edu.

[⊥] **Author Contributions**

M.S.D., S.P., and M.G. contributed equally.

Present Address: Department of Biochemistry, University of Washington, HSB J367, 1959 NE Pacific Street, Seattle, Washington 98195, United States. (M.S.D.)

Complete contact information is available at: https://pubs.acs.org/10.1021/acs.biochem.1c00654

Accession Codes

The AKT1 protein sequence from *A. thaliana* (AKT1_AR-ATH) was taken from UniProt accession UniProtKB - Q38998. The atomic coordinates for AtAKT1 have been deposited in the PDB (accession: 7T4X), and the associated EM volumes have been deposited in the EMDB (accession: EMD-25691).

The authors declare no competing financial interest.

We determined structures of the hyperpolarization-activated channel AKT1 from *Arabidopsis thaliana*, which mediates K^+ uptake from the soil into plant roots. These structures of AtAKT1 embedded in lipid nanodiscs show that the channel undergoes a reduction of C4 to C2 symmetry, possibly to regulate its electrical activation.

I on channels in plants perform a number of critical physiological tasks including the uptake of nutrients from the soil for plant development and viability, regulation of turgor pressure to control mechanical processes, and action potential-like electrical signaling.[1–3] Among the most important nutrients for plants is K^+, for which there exist numerous validated channel genes in the model organism *Arabidopsis thaliana*[1,3] including 6-transmembrane helix (TM) *Shaker*-like channels, 12-TM two-pore channels, 4-TM twin pore channels, and 2-TM K_{ir} channels.[1,2] The AKT1 channel is necessary for radial K^+ transport, where it mediates the translocation of K^+ from the rhizosphere into the root hair, from which the ion can diffuse through an outwardly rectifying Stelar K+ outward rectifying (SKOR) channel into the xylem for transport across the plant shoot.[1,4,5] The *Arabidopsis thaliana akt1* gene —first discovered by phenotypic rescue of K^+ uptake-deficient yeast[6]—encodes a 96 990 Da α subunit that assembles into a homotetrameric channel. The protein contains five distinct domains: (1) a Shaker-like transmembrane cassette consisting of TM helices S1–S4 (constituting the voltage sensing domain) and S5–S6 (the pore domain); (2) an extended helical C-linker; (3) a cyclic nucleotide binding homology domain (CNBHD); (4) an ankyrin repeat domain; and (5) a C-terminal K_{HA} interaction domain.

In contrast to other putative cyclic nucleotide binding channels, AKT1 is unlikely to be regulated by cyclic nucleotide monophosphates (cNMPs), as it lacks critical residues for ligand binding that are present in bona fide cyclic nucleotide binding domains (CNBDs)[7] (Figure S4). Instead, channel gating is voltage-dependent and modulated by a phosphorylation “switch”.[1,3,8–10] Yeast two-hybrid experiments show that the AKT1 ankyrin repeat domain associates with a CIPK23 kinase/calcineurin B-like (CBL) calcium sensor complex, and patch clamp recording of current in *X. laevis* oocytes confirms that phosphorylation by this complex converts a nearly silent channel to a strongly hyperpolarization-activated channel with an activation threshold of ~−50 mV.[8] Conversely, AKT1 can be inhibited by direct interaction with CBL10 or dephosphorylation by PP2C phosphatases.[8,11] Phosphorylation couples channel activity, and thus K^+ uptake, to intricate Ca^{2+} signaling networks in order for the plant to adapt to a range of soil conditions. Additionally, AKT1 is known to hetero-oligomerize with the pseudochannel KC1, negatively shifting its $V_{1/2}$ by ~60 mV.[11] These modifications and interactions are critical for plant viability: activating modifications are necessary to facilitate the influx of K^+ against large concentration gradients when $[K^+]_{soil}$ is low, and inhibition is needed to prevent K^+ leakage out of the roots when E_K is below V_m.

Here, we determined the structure of AKT1 from *A. thaliana* by single-particle cryogenic electron microscopy (cryoEM) (Figure 1A,B). We reconstituted AKT1 into soy polar lipid nanodiscs and determined a C2-symmetric consensus structure to an average resolution of 2.8 Å. We observe a reduction of symmetry from the predicted C4 to C2, occurring in regions of the protein with known functional significance, namely the C-linker and

CNBHDs. Heterogenous image processing of the consensus refinement reveals that the CNBHDs are highly mobile domains that flex about the channel axis and that the C-linker alternates between two distinct conformations. Although the electrophysiological implications of these observations are yet to be determined, we suspect that similar processes may occur in other channels from the CNG and hyperpolarization-activated families.

The overall architecture of the AKT1 channel is similar to other non-domain-swapped ion channels such as the hyperpolarization-activated HCN1,[12,13] KAT1,[14] and LliK[15] channels, the depolarization-activated ether-a-go-go channel,[16] and the ligand-gated CNGA1 channel.[17] In these channels, the S4 helix from the voltage sensing domain (VSD) that bears the gating charges is linked to the S5 helix of the pore domain via a short loop (Figure 1A) such that the pore and voltage sensing domains of the same subunit coalesce together as a bundle. This is in contrast to the canonical domain swapped architecture found in *Shaker*-like, Na_V, and two-pore channels, in which the VSD and pore helices are separated by a long helical S4–S5 linker.[13] Our structure is consistent with a deactive, closed channel, in which the gating charges on S4 are in a resting, "up" position (Figure 1C), and the intracellular activation gate is constricted to preclude the diffusion of ions through the central pore (Figure 1D). Previous work on the hyperpolarization-activated HCN1 channel showed that two gating charges are transferred downward across the hydrophobic constriction site (HCS) during activation, accompanying a helical break in S4.[13] In our structure, the corresponding charges are R164 and R167, which rest above the HCS formed by F100, while R169 and R170 are below the HCS closely interacting with an intracellular negative cluster formed by E61, D103, and D139 (Figure 1C).

The selectivity filter of AKT1 is nearly identical to all other K^+-selective channels of known structure, consisting of a tetrameric "bracelet" arrangement of backbone carbonyls from the signature TVGYG motif (Figure 1F), mimicking the eight-water-ligand field around K^+ ions in bulk solvent[18,19] (Figure 1D,E). We assign four K^+ ions to densities on the channel axis within the selectivity filter, which correspond to superpositions of alternately populated pairs of sites (Figure 1E). In addition, we observe a crown of four extracellular water molecules partially hydrating an S_0 K^+, which are possibly hydrogen-bonded to histidine residues (H260), conserved in plant inwardly rectifying K^+ channels (Figure S5A,B)[20] that line the extracellular face of the channel. In this model, H260 donates a hydrogen bond from its δ nitrogen to its own backbone carbonyl, poising it is putatively unprotonated ε nitrogen toward a crown water proton, thus aligning the water toward the S_0 K^+ (Figure S5A,B). The H260 imidazoles may facilitate partial dehydration of incoming $K^+ \cdot (H_2O)_8$ complexes by positioning the hydration crown, allowing the K^+ to transition into a partially hydrated state (i.e., $K^+ \cdot (H_2O)_4(C{=}O)_4$) above the selectivity filter. Below the selectivity filter is an aqueous bath where K^+ ions can rehydrate, followed by an intracellular activation gate wherein the side chains of I285 and T289 form an ion-excluding constriction point (Figure 1D).

Initial image processing with imposition of C4 symmetry showed high-resolution features in the transmembrane domain, including an abundance of annular phospholipids, K^+ ions in the selectivity filter, and pore waters, but smeared density corresponding to intracellular domains. For this reason, we reperformed all 3D image processing without

imposition of symmetry, and also, fourfold symmetry expanded the consensus C4 particle stack. Subsequent 3D classification produced multiple conformations of the channel, each exhibiting a dramatic reduction of symmetry from four to twofold. Intriguingly, we observe the C-linker, which links the pore domain to the CNBHD, in two distinct configurations on the same C2-symmetric reconstruction. Neighboring AKT1 subunits adopt alternating C-linker conformations: the first conformation is termed “flat”, similar to that observed in the published structures of LliK[15] and HCN1,[12] whereas the second conformation is termed “kinked” and resembles that of KAT1.[14] Variations in C-linker and CNBD/CNBHD architecture have been observed between different channels, though the exact nature of these differences is not always clear.[7,12,14,15,17,21] Our structures suggest that these channels may sample multiple conformations during their respective activation cycles and that there may be direct implications for regulation of electrical activation (Figure 2A–D).

In the kinked conformation, the C-linker forms an intricate interaction nexus with S6 and its neighboring protomer’s VSD (Figure 2A). D337 is situated at the summit of the kink and forms an apparent salt bridge with R298 on S6. Y334 forms H-bonds with K180 at the bottom of S4 and R298 and also an aryl stacking interaction with F302 on S6. Furthermore, the kink appears to be stabilized by a close interaction between K333 and E339 from the C-linker itself. In the flat conformation, this nexus is significantly altered due to the intercalation of an N-terminal helix that precedes S1 (Figure 2A,B). This N-helix is only observed above the flat C-linker, where it makes extensive contacts with S6, the VSD, and the C-linker. The linkage between the N-helix and S1 is not resolved; yet, we are able to confidently model a 12 amino acid stretch that well-satisfies the EM density and chemical environment (Figures 2D and S2D).

In the flat conformer, the aryl interaction between Y334 and F302 is largely broken as are the salt bridges between K333/E339 and D338/R298, as D337 is forced to face away from S6 (Figure 2A,E). Although the exact functional consequence of these differences is still unclear, we propose that the insertion of the N-helix serves to autoregulate the electrical activation of S4. In order to activate the channel, S4 must translocate downward to some extent,[13,14,22] and the presence of the N-helix between it and the C-linker may sterically occlude this process (Figure 2B). The N-helix makes extensive contacts with the VSD, S6, and C-linker (Figure 2D). D18 forms an electrostatic bridge between K115 on the S2–S3 loop and K180 on the S4–S5 loop. E19 forms a salt bridge with R335 on the C-linker, and a multitude of van der Waals interactions are satisfied between the N-helix, S6, and C-linker (Figure 2D). Finally, we observe strong continuous density between C13 and C331 from the C-linker, suggesting that the N-helix may be covalently stapled to the C-linker (Figures 2A,D and S2D).

Asymmetry is further observed in subsequent domains. The CNBHD that follows the flat C-linker is notably flexible, whereas the postkinked CNBHD is resolved to high resolution, allowing for accurate atomic structure determination. As a result of this asymmetry, the inter-CNBHD interactions around the channel ring differ considerably. Focused classification on the CNBHD domains from the original C1 particle stack of EM images without imposition of symmetry recovered three distinct states. The first of these has apparent C4 symmetry, while the latter two have varying degrees of C2 symmetry (Figure

2E). At low-contour levels, the ankyrin domains are also seen to adopt a strongly elongated C2 symmetric configuration, in which two adjacent pairs of ankyrin domains form close contacts with one another, leaving a gap between these and the alternate pair of domains (Figure 2F). As the channel was heterologously expressed in mammalian cells without a CIPK/CBL10 phosphorylation system, we assume that the ankyrin domains are unmodified. Therefore, it is feasible that ankyrin phosphorylation alters this configuration for channel activation, possibly by breaking apart these inter-Ankyrin interactions to symmetrize the channel.

Although the precise role of symmetry breaking in a degenerate ligand-binding domain remains unclear, our results suggest that it might serve a regulatory role. The observed differences between adjacent CNBHD conformations is reminiscent of the transition between apo- and cNMP-bound states of cyclic nucleotide-gated ion channels (Figure 2C,D), posing the possibility that this domain in AKT1 has been converted from a ligand-binding domain to a site of allosteric communication between the ankyrins and the channel's pore. It is enticing to compare our observations with those of other CNBHD-containing channels whose electrical properties are altered by N- and C-terminal regulatory domains. In the case of hERG, an N-terminal helix acts in concert with the CNBHD to enhance the channel's activation kinetics and mar its speed of deactivation.[23,24] In the depolarization-activated hERG channel, insertion of an N-terminal helix between its C-linker and VSD would, according to our model, "push" the S4 helix upward toward an activated conformation and prevent its deactivation into a resting, downward state. Inversely, downward translocation of S4 during activation in a hyperpolarization-activated channel such as AKT1 would be inhibited by the presence of such a helix. We hope that the unusual findings presented in this manuscript will help inform experiments on this very important plant channel and on the many salient hyperpolarization- and CNBD-containing channels in human physiology.

Supplementary Material

Refer to Web version on PubMed Central for supplementary material.

ACKNOWLEDGMENTS

We thank Phuong Nguyen for assistance with mammalian cell culture. We thank David Bulkley, Glen Gilbert, and Zanlin Yu for their maintenance of the UCSF electron microscopy core and the NIH grants that support them. We thank Paul Thomas, Matt Harrington, Joshua Baker-LePain, and the Wynton HPC team for computational advice and support. We thank Janet Finer-Moore, Evan Green, and Richard Aldrich for critical reading of the manuscript. M.S.D. acknowledges an NSF graduate research fellowship. Research was supported by NIH grant GM24485 (to R.M.S.).

REFERENCES

(1). Hedrich R Ion channels in plants. Physiol. Rev 2012, 92, 1777–1811. [PubMed: 23073631]

(2). Ward JM; Mäser P; Schroeder JI Plant ion channels: gene families, physiology, and functional genomics analyses. Annu. Rev. Physiol 2009, 71, 59–82. [PubMed: 18842100]

(3). Sharma T; Dreyer I; Riedelsberger J The role of K(+) channels in uptake and redistribution of potassium in the model plant Arabidopsis thaliana. Front. Plant Sci 2013, 4, 224. [PubMed: 23818893]

(4). Hirsch RE; Lewis BD; Spalding EP; Sussman MR A role for the AKT1 potassium channel in plant nutrition. Science 1998, 280, 918–921. [PubMed: 9572739]

(5). Li J; et al. The Os-AKT1 channel is critical for K+ uptake in rice roots and is modulated by the rice CBL1-CIPK23 complex. Plant Cell 2014, 26, 3387–3402. [PubMed: 25096783]

(6). Anderson JA; Huprikar SS; Kochian LV; Lucas WJ; Gaber RF Functional expression of a probable Arabidopsis thaliana potassium channel in Saccharomyces cerevisiae. Proc. Natl. Acad. Sci. U.S.A 1992, 89, 3736–3740. [PubMed: 1570292]

(7). Matulef K; Zagotta WN Cyclic nucleotide-gated ion channels. Annu. Rev. Cell Dev. Biol 2003, 19, 23–44. [PubMed: 14570562]

(8). Lee SC; et al. A protein phosphorylation/dephosphorylation network regulates a plant potassium channel. Proc. Natl. Acad. Sci. U.S.A 2007, 104, 15959–15964. [PubMed: 17898163]

(9). Hedrich R; Kudla J Calcium signaling networks channel plant K+ uptake. Cell 2006, 125, 1221–1223. [PubMed: 16814705]

(10). Xu J; et al. A protein kinase, interacting with two calcineurin B-like proteins, regulates K+ transporter AKT1 in Arabidopsis. Cell 2006, 125, 1347–1360. [PubMed: 16814720]

(11). Ren X-L; et al. Calcineurin B-like protein CBL10 directly interacts with AKT1 and modulates K+ homeostasis in Arabidopsis. Plant J 2013, 74, 258–266. [PubMed: 23331977]

(12). Lee C-H; MacKinnon R Structures of the Human HCN1 Hyperpolarization-Activated Channel. Cell 2017, 168, 111–120.e11. [PubMed: 28086084]

(13). Lee C-H; MacKinnon R Voltage Sensor Movements during Hyperpolarization in the HCN Channel. Cell 2019, 179, 1582–1589.e7. [PubMed: 31787376]

(14). Clark MD; Contreras GF; Shen R; Perozo E Electromechanical coupling in the hyperpolarization-activated K+ channel KAT1. Nature 2020, 583, 145–149. [PubMed: 32461693]

(15). James ZM; et al. CryoEM structure of a prokaryotic cyclic nucleotide-gated ion channel. Proc. Natl. Acad. Sci. U.S.A 2017, 114, 4430–4435. [PubMed: 28396445]

(16). Whicher JR; MacKinnon R Structure of the voltage-gated K^+ channel Eag1 reveals an alternative voltage sensing mechanism. Science 2016, 353, 664–669. [PubMed: 27516594]

(17). Xue J; Han Y; Zeng W; Wang Y; Jiang Y Structural mechanisms of gating and selectivity of human rod CNGA1 channel. Neuron 2021, 109, 1302–1313.e4. [PubMed: 33651975]

(18). Zhou Y; Morais-Cabral JH; Kaufman A; MacKinnon R Chemistry of ion coordination and hydration revealed by a K+ channel-Fab complex at 2.0 A resolution. Nature 2001, 414, 43–48. [PubMed: 11689936]

(19). Morais-Cabral JH; Zhou Y; MacKinnon R Energetic optimization of ion conduction rate by the K+ selectivity filter. Nature 2001, 414, 37–42. [PubMed: 11689935]

(20). Hoth S; et al. Molecular basis of plant-specific acid activation of K+ uptake channels. Proc. Natl. Acad. Sci. U.S.A 1997, 94, 4806–4810. [PubMed: 9114073]

(21). Li M; et al. Structure of a eukaryotic cyclic-nucleotide-gated channel. Nature 2017, 542, 60–65. [PubMed: 28099415]

(22). Dai G; Aman TK; DiMaio F; Zagotta WN The HCN channel voltage sensor undergoes a large downward motion during hyperpolarization. Nat. Struct. Mol. Biol 2019, 26, 686–694. [PubMed: 31285608]

(23). Muskett FW; et al. Mechanistic insight into human ether-á-go-go-related gene (hERG) K+ channel deactivation gating from the solution structure of the EAG domain. J. Biol. Chem 2011, 286, 6184–6191. [PubMed: 21135103]

(24). Gustina AS; Trudeau MC hERG potassium channel gating is mediated by N- and C-terminal region interactions. J. Gen. Physiol 2011, 137, 315–325. [PubMed: 21357734]

(25). Pravda L; et al. MOLEonline: a web-based tool for analyzing channels, tunnels and pores (2018 update). Nucleic Acids Res 2018, 46, W368–W373. [PubMed: 29718451]

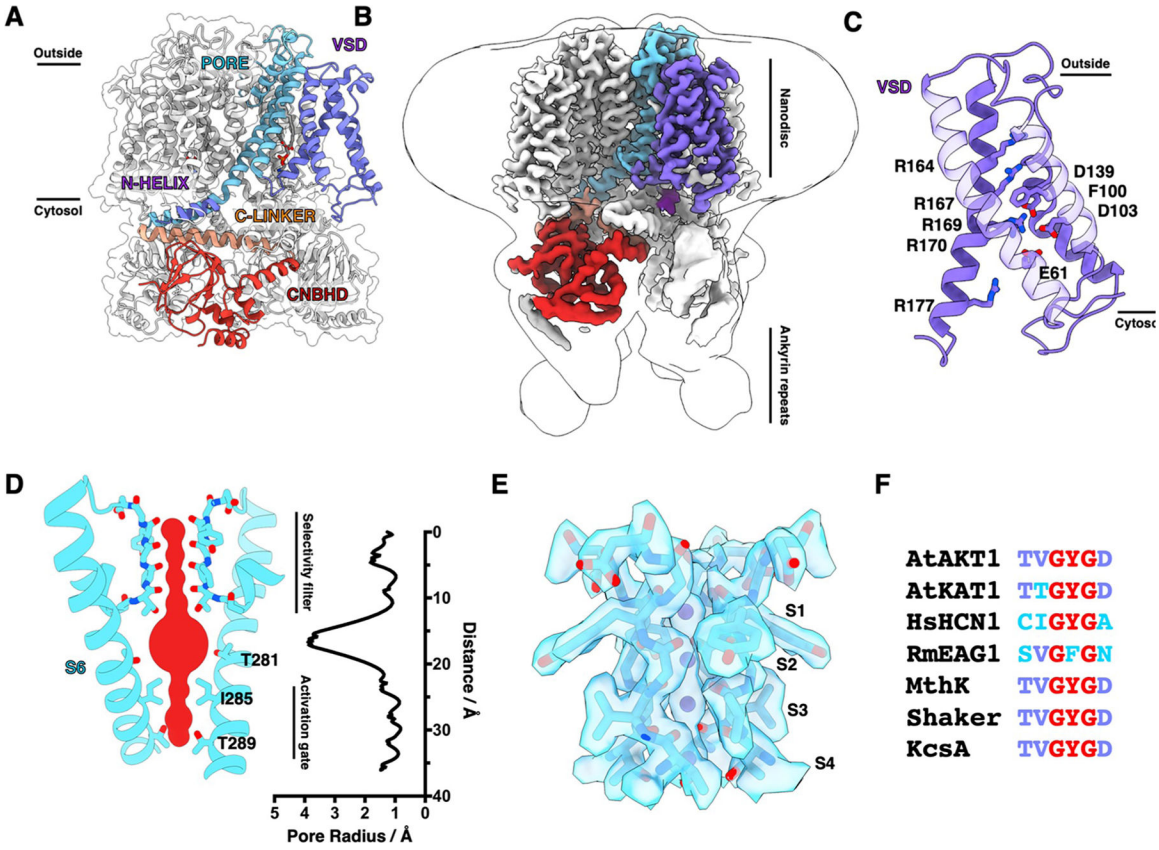

Figure 1.

CryoEM structure and functional state of AtAKT1 in a lipid bilayer. (A) Molecular model of the AtAKT1 homotetramer with a single subunit colored by domain. (B) Sharpened electrostatic potential map, colored by domain as in (A) with low-pass filtered envelope shown to depict the nanodisc and poorly resolved ankyrin repeats. (C) The deactive voltage sensing domain with charge transfer center residues shown. (D) Pore profile of the closed channel with pore-lining residues on the P-loop and S6 shown including the selectivity filter near the extracellular side, and activation gate at the intracellular side. The pore radius is shown plotted with respect to the distance along the channel axis, calculated using MOLE.[25] (E) Atomic model of the selectivity filter and K^+ ion superpositions, with sharpened electrostatic potential map shown zoned 2.5 Å around the atoms of interest. (F) Residues that form the selectivity filter from AtAKT1 and other K^+ channels, highlighting the signature GYG motif.

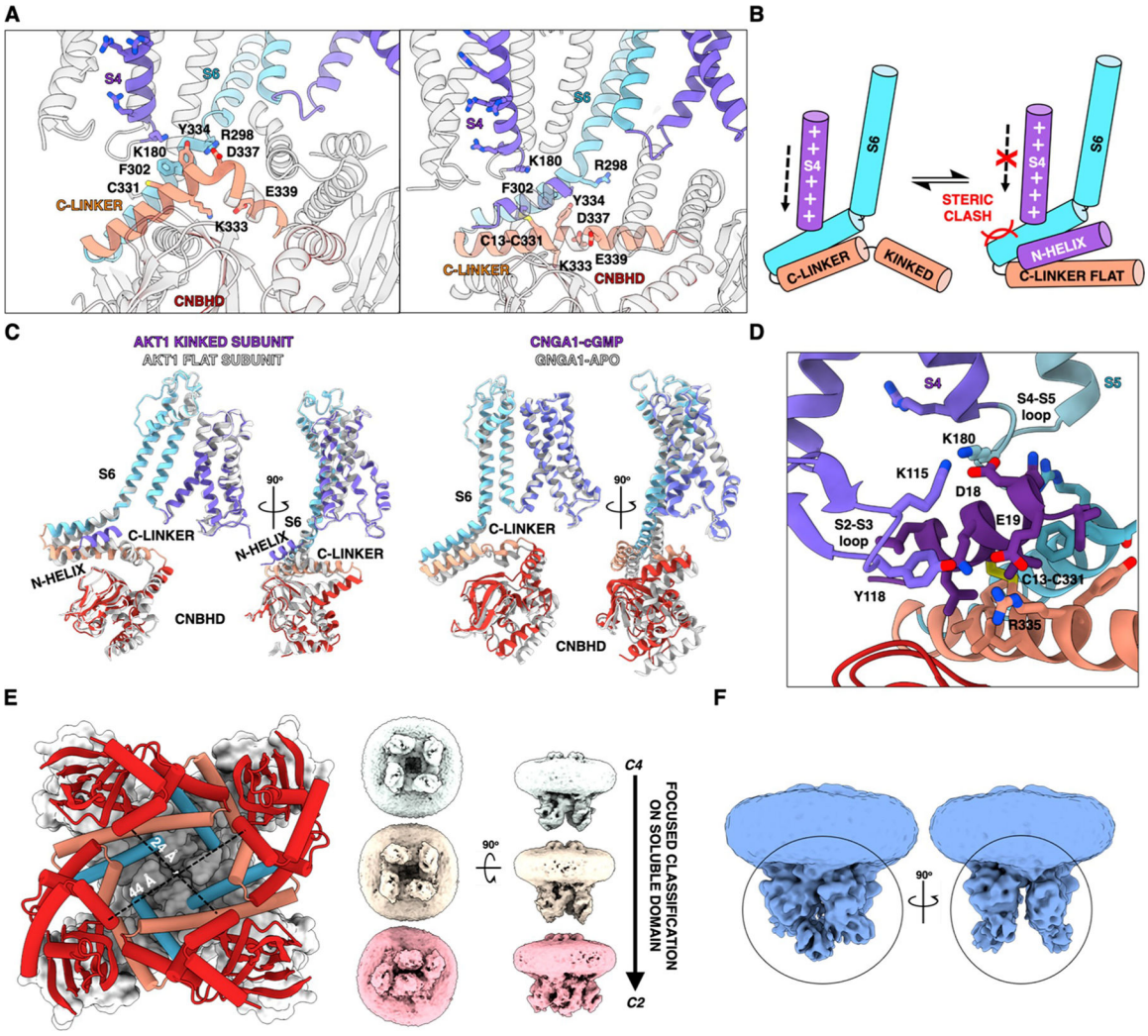

Figure 2.

Symmetry reduction in AtAKT1 and its implications for voltage activation. (A) The C-linker adopts two different conformations in the C2-symmetric structure. In one conformation, the linker is kinked (left box), forming a nexus with S4 and S6. In the adjacent subunit, the C-linker is flattened by insertion of the pre-VSD N-terminal helix, breaking most atomic interactions in the nexus (right box). (B) Graphical model of how N-helix insertion flattens the C-linker (represented by solid arrows) and potentially interferes with the downward translocation of S4 during membrane hyperpolarization (represented by dashed arrows). (C) Orthogonal views of overlaid AKT1 kinked and flat subunits (left), and apo- and holo-CNGA1 (right) (PDBs: 7LFT and 7LFW, respectively) highlighting differences in C-linker and CNBD conformations. (D) Atomic interactions between the N-helix, VSD, C-linker, and pore domain. (E) Three conformations of the CNBHD domains are recovered from 3D classification (right), the C4 class at ~2.6 Å displayed at top, mid-C2 class at ~2.8 Å in the center (used for model building and atomic interpretation), and ultra-C2 class at ~4.5 Å on the bottom, all viewed at low contour. The soluble region in the mid-C2 class was resolved to high resolution and was used to build an atomic model of AKT1, shown on the left. The

degree of asymmetry is quantified by the distances between D337 on opposite C-linkers. (F) Orthogonal views of the mid-C2 map, displayed at low contour to show the ankyrin domains in two distinct configurations: one pair exhibits extensive interdomain interactions, while the neighboring pair does not touch.